Propagation of Lamb waves in a plate with a periodic grating: Interpretation by phonon

Damien Leduc[a)]
Laboratoire d'Acoustique Ultrasonore et d'Electronique, UMR CNRS 6068, Université du Havre, Place Robert Schuman, BP 4006, 76610 Le Havre, France

Anne-Christine Hladky
Institut d'Electronique de Microélectronique et de Nanotechnologie, UMR CNRS 8520, 41 boulevard Vauban, 59046 Lille, France

Bruno Morvan, Jean-Louis Izbicki, and Pascal Pareige
Laboratoire d'Acoustique Ultrasonore et d'Electronique, UMR CNRS 6068, Université du Havre, Place Robert Schuman, BP 4006, 76610 Le Havre, France

(Received 11 February 2005; revised 20 June 2005; accepted 30 June 2005)

In this paper the propagation of Lamb waves in an aluminium plate with a periodic grating containing triangular grooves is studied. Numerical simulations (FEM) are performed. A single incident mode is excited on a flat area and the interaction with the periodic grating is studied. Reflected converted waves are observed when the incident Lamb wave passes through the grating. At the entrance of the periodic grating, a phonon relation is written between the incident signal, the converted mode, and the phonon related to the grating. An experimental verification of the phonon relation is carried out. © *2005 Acoustical Society of America.* [DOI: 10.1121/1.2005987]

PACS number(s): 43.35.Cg, 43.20.Mv [ANN] Pages: 2234–2239

I. INTRODUCTION

Ultrasonic waves are sensitive to surface roughness. Ultrasonic reflection and transmission at a rough fluid-solid interface have been widely dealt with in the past.[1,2] In particular, surface roughness characterization is a subject of great interest for bonded structures. Indeed, the bonding surface is often roughened before applying glue in order to improve the bonding quality. In this study in order to characterize the roughness of internal interfaces, we use guided Lamb-type waves which are well-suited to this purpose, contrary to surface waves (Rayleigh or Scholte).

Few studies concern the propagation and the scattering characteristics of guided waves in plates with rough surfaces. Lobkis *et al.*[3,4] have developed a model from the phase-screen approximation (PSA). Thanks to this model, the damping of Lamb waves by the interaction of partial waves (shear and compressional) with the rough surface can be explained. For rough surfaces, a usual characteristic parameter is the value of the root mean square roughness height R_q.[5] In Refs. 3 and 4, the Lamb wave damping is a function of R_q. Potel *et al.*[6,7] consider the problem with a perturbation approach; this approach also supposes restriction on the R_q value and it is assumed that the surface profile varies slowly. This model also provides for the Lamb wave the real and imaginary parts of the wave number. Whatever the model considered, the real part of the wave vector, and thus the wavelength λ, of the Lamb wave is not sensitive to the presence of roughness at least for the studied R_q values. The imaginary part of the wave vector (i.e., damping) in Ref. 6 is related both to the value of R_q and the spatial distribution of the roughnesses. From an experimental point of view, a power spectral density performed on a roughness profile shows dominant wavelengths Λ (spatial period). Indeed, a rough surface may be regarded as made up of a combination of several spatial periods with different wavelengths. For a given measured damping of one Lamb mode, it is possible to fit the result with one of the spatial periods present on the sample. The question is now how to choose the most influential spatial period Λ among them. In order to answer this question, it is important to find the condition between the wavelength λ of the Lamb mode and the different spatial periods Λ to obtain their interaction. To further comprehend this interaction, the study of a periodical grating made of identical groves is proposed. In the past, previous studies on periodical gratings have mainly concerned surface waves by means of the Rayleigh wave.[8–10] The main result is that the diffraction of the Rayleigh wave obeys a Bragg relation. The Scholte wave can also be diffracted by a grating.[8,11–13] In this paper, we present numerical and experimental results on Lamb waves propagating on a grooved surface, because the work is dedicated to the control of surface bonding. To the authors' knowledge, there is no recent work which deals with the propagation of Lamb waves on a plate with a surface grating. This paper shows that when a Lamb wave is incident on a periodical grating, reflected converted modes appear at particular frequencies. This result can be interpreted as a consequence of phonon interaction. Therefore, a relation between incident and converted mode wave numbers and the grating period Λ is established. This relation results from the law of conservation of phonon momentum.

First, after a brief description of the samples, numerical simulations are presented. Signal processing allows us to give an interpretation of the results in the dual space (wave-

a)Electronic mail: damien.leduc@univ-lehavre.fr

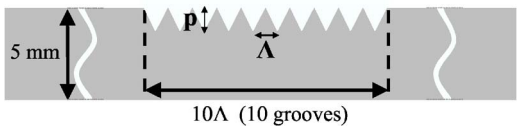

FIG. 1. Geometry of the studied samples.

number/frequency space). Several examples with various spatial periodicities are presented with a view to illustrating physical phenomenona, such as conversion modes, depth effect, and so on. Finally, an experimental study validating the numerical results is carried out.

II. NUMERICAL SIMULATIONS

A. Description of the studied samples

The studied samples are aluminium plates. Only a part of one side is treated with ten identical triangular grooves. This surface treatment can be found on only one side because the aim of this work will be to study the quality of a bonded structure with a rough interface. The other side of the plate is not treated and stands as a reference surface.

The grooves have a depth p and a spatial periodicity Λ (Fig. 1). The plates are 5 mm thick. The acoustics parameters, longitudinal and shear velocities, are respectively $c_L = 6320$ m/s and $c_T = 3115$ m/s. The density of the aluminium is equal to 2700 kg/m.

B. Numerical processing

The ATILA® finite element code was developed in the Acoustics Department of ISEN-France, for the modeling of sonar transducers.[14] It permits the static, modal, harmonic, and transient analysis of unloaded elastic, piezoelectric, or magnetostrictive structures, as well as the harmonic or transient analysis of radiating elastic or piezoelectric structures. It is able to analyze axisymmetrical, bi- or three-dimensional structures.

A transient analysis is performed to study the propagation of Lamb waves on a plate with a periodic grating. Because the plate is supposed to be infinite in one direction, a bi-dimensional mesh is used, using a plane strain condition. The plate is meshed and divided into elements connected by nodes. Isoparametric elements are used, with a quadratic interpolation along element sides. The elastic plate is submitted to analytical displacements on one edge of the plate with a view to exciting the S_0 Lamb mode. Then a Fourier transform clearly verifies that only the S_0 Lamb mode is excited. At a frequency of 800 kHz, a burst of five sinusoids is used. At this frequency, the wavelength of this Lamb mode is $\lambda = 3.75$ mm. The mesh must be long enough before and after the grating to avoid parasitic reflections on the edges. Transient analysis is then performed during 60 periods (75 μs), with a 0.05-μs time interval. Various meshes are considered: the spatial periodicity of the grooves varies from 2 to 3.9 mm. The grooves are supposed to all be identical with a depth of p. Computations provide the displacement at each node and at each time interval. In particular, the normal displacement before and after the grating are studied and time-space diagrams are drawn.

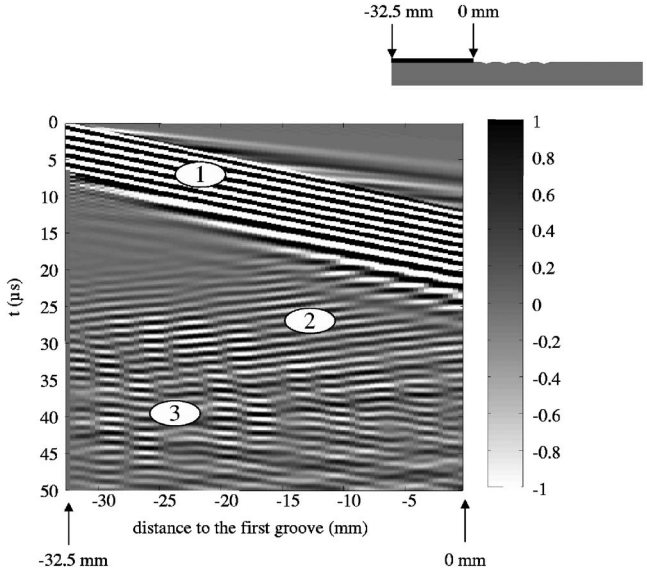

FIG. 2. Representation of the signal in the (x,t) space for a plate with a grating. The grating contains ten grooves. The spatial periodicity is $\Lambda = 2.4$ mm and the groove depth is equal to $p = 100$ μm. The origin of the spatial coordinate is the first groove. The levels of the incident signal are saturated in order to visualize the reflected signal.

C. Results

In Fig. 2, a time-space image of the normal surface displacements is given in the case of a grating with periodicity $\Lambda = 2.4$ mm. In the gray scale, the amplitude of the displacements of the surface located before the grating is represented. The zero of the spatial coordinate is fixed at the entrance of the grating. In this figure the gray scale is saturated in order to visualize the reflected signal whose amplitude is weaker than the incident signal. The depth of the grooves is $p = 100$ μm. Three parts of the signal are observed (Fig. 2): the incident signal (1), the reflection from the grating (2), and the reflection from the left edge of the plate (3). In this figure, it is shown that reflected waves appear on each groove. This explains the apparent temporal spreading of the reflected wave.

Reflected and incident waves are separated by applying a 2D FFT on the signals (Fig. 3). This calculation leads to a dual representation in the wave-number/frequency space (k,f). Positive components of wave number k correspond to the incident waves [Fig. 3(a)] whereas negative wavenumber values correspond to reflected waves [Fig. 3(b)]. Thus we can verify that the S_0 Lamb wave is properly excited on the plate. The theoretical S_0 dispersion curve is superimposed on the experimental signal. The signal excitation described in the previous paragraph explains why there is a spreading of the frequency bandwidth around a frequency of $f = 800$ kHz. According to Fig. 3(a), the main lobe of the frequency excitation extends from 660 to 920 kHz. This is not a problem because signal analysis is performed in dual space and each frequency component can be dealt with independently. Figure 3(b) shows a converted A_1 wave reflected from the grating. This wave is precisely located at frequency $f = 760$ kHz.

The FEM analysis is repeated for a grating with spatial periodicity Λ varying from 2 to 3.9 mm by 0.1 mm step.

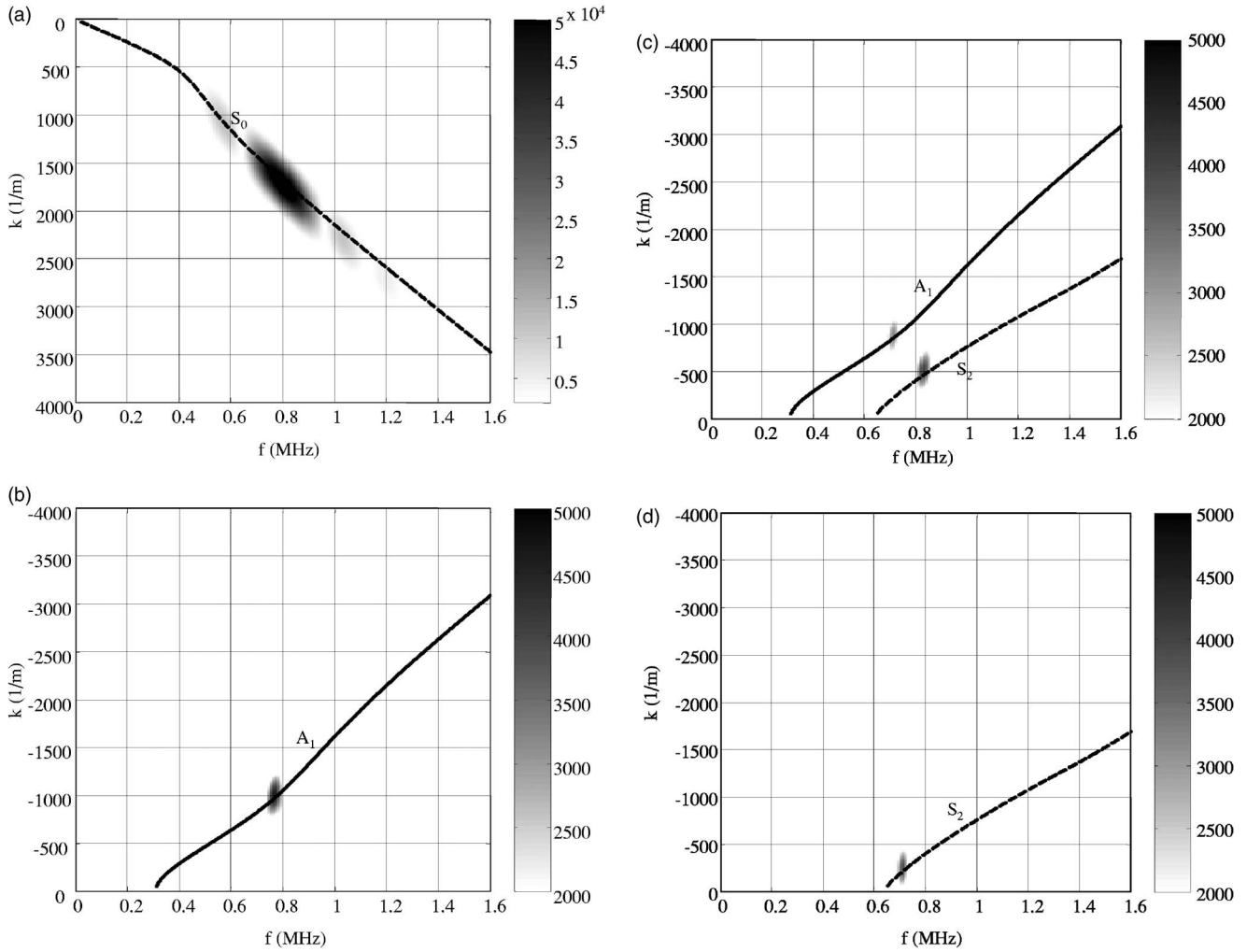

FIG. 3. Representation of the signal in dual space (k,f). The grating contains ten grooves. The grooves depth p is equal to 100 μm. (a) is the incident signal. The spatial periodicity is equal to (b) $\Lambda=2.4$ mm, (c) $\Lambda=2.7$ mm, and (d) $\Lambda=3.7$ mm. The lines correspond to the theoretical dispersion curves: solid line for A_1 mode and dotted lines for S_2 mode. Gray levels are fixed in order to compare the signals.

Two-dimensional fast Fourier transforms (2D FFTs) are carried out on the time-space signals for each value of Λ. Figures 3(b)–3(d) show that converted modes S_2 or/and A_1 can be seen at different frequencies. For instance, if $\Lambda=2.4$ mm [Fig. 3(b)], the conversion appears at $f=760$ kHz. At this frequency, the wave number for the A_1 converted mode is equal to 1010 m^{-1} and the wave number for the S_0 incident mode is equal to 1610 m^{-1}. The quantity $2\pi/\Lambda$ is homogeneous to a wave number and is a characteristic of the grating in dual space. For $\Lambda=2.4$ mm, $2\pi/\Lambda$ is equal to 2617 m^{-1}. One can notice that if we add the values of the incident and converted wave numbers ($k_{S0}=k_{S2}=2620$ m^{-1}), the obtained value is approximately $2\pi/\Lambda$ (relative error: 0.1%). This relation is verified for each grating periodicity and results are presented in Table I. This relation can be interpreted as a phonon relation and is described in detail in the next section.

III. INTERPRETATION: THE PHONON RELATION

The equality obtained in the previous section is in fact a relation between phonons. The S_0 incident mode is converted into S_2 or A_1 mode at the entrance of the grating. The scattering process occurring at the entrance can be described as a collision of phonons. The law of conservation of the phonon momentum can be written as

$$\mathbf{p}_{S0} = \mathbf{p}_{PH} + \mathbf{p}_{CM}, \tag{1}$$

where the converted mode (CM) propagates in the opposite direction to the S_0 incident mode. The phonon (PH) propagates under the grating in the direction of propagation of the incident wave. This implies a relation between the wave numbers:

$$k_{S0} = \frac{2\pi}{\Lambda} - k_{CM}. \tag{2}$$

Here we can recognize the relation which was verified in Table I with a maximum relative error of 3.4%. The incident and reflected waves verify a Bragg-type relation. Indeed, Eq. (2) can also be interpreted as a phase matching. The converted waves excited on two successive grooves must be in phase and the phase matching which corresponds to the smaller path implies

TABLE I. Comparison between the sum of the incident (k_{S0}) and converted wave numbers (k_{S2} or k_{A1}) and the phonon wave number related to the grating ($2\pi/\Lambda$). The column "frequency" corresponds to the frequency where the conversion is at a maximum.

Λ (mm)	$2\pi/\Lambda$ (m^{-1})	k_{S2} (m^{-1})	k_{S0} (m^{-1})	k_{A1} (m^{-1})	Frequency (kHz)	Σk (m^{-1})	Relative error
2	3140		1840	1260	850	3100	1.3%
2.1	2992		1770	1170	820	2940	1.7%
2.2	2856		1720	1115	805	2835	0.7%
2.3	2732		1670	1050	785	2720	0.4%
2.4	2618		1620	1000	765	2620	0.1%
2.5	2513		1570	955	745	2525	0.5%
2.6			1545	930	725	2475	2.4%
	2417	565	1845	845	2410	0.3%	
2.7			1490	885	710	2375	2.1%
	2327	520	1795	830	2315	0.5%	
2.8			1435	840	695	2275	1.4%
	2244	480	1745	815	2225	0.8%	
2.9	2167	460	1720		795	2180	0.6%
3	2094	420	1670		785	2090	0.2%
3.1	2027	400	1645		770	2045	0.9%
3.2	1963	380	1620		760	2000	1.9%
3.3	1904	355	1590		750	1945	2.2%
3.4	1848	330	1570		740	1900	2.8%
3.5	1795	310	1545		730	1855	3.3%
3.6	1745	290	1515		720	1805	3.4%
3.7	1698	260	1490		715	1750	3.1%
3.8	1653	240	1460		705	1700	2.8%
3.9	1611	220	1440		695	1660	3.0%

$$k_{S0} \cdot \Lambda + k_{CM} \cdot \Lambda = 2\pi. \quad (3)$$

Thus the physical problem of the interaction between the Lamb waves and the grating can be considered in dual space as a phonon process, and in direct space as an interference process involving a phase matching.

New curves can be plotted to predict the possible conversion. On the Lamb wave, k_{CM} values are superimposed on the theoretical Lamb waves dispersion curves for a free plate (Fig. 4). These curves are plotted for values of Λ varying from 2 to 3.9 mm. The intersections give the possible converted modes for a given grating. For instance, if the spatial periodicity of the grating is $\Lambda=3$ mm, intersections between the phonon relation curve and the dispersion curves give a predicted conversion into S_2 mode at $f=800$ kHz. This mode is effectively observed at $f=785$ kHz (Table I—relative error: 1.9%). S_1 mode is also a potential converted mode in the frequency bandwidth, at lower frequency, but the normal displacement of this mode is too weak on the surface and thus it is not possible to detect it.[10] There are other intersections but most of them are out of the frequency bandwidth of excitation.

At the exit of the grating we have verified that only the S_0 mode is propagating and consequently the phonon relation Eq. (1) is also valid.

The grating can also be characterized by the depth of the grooves. To see if this parameter influences the phonon relation, a parametric study of a grating with various depths is carried out.

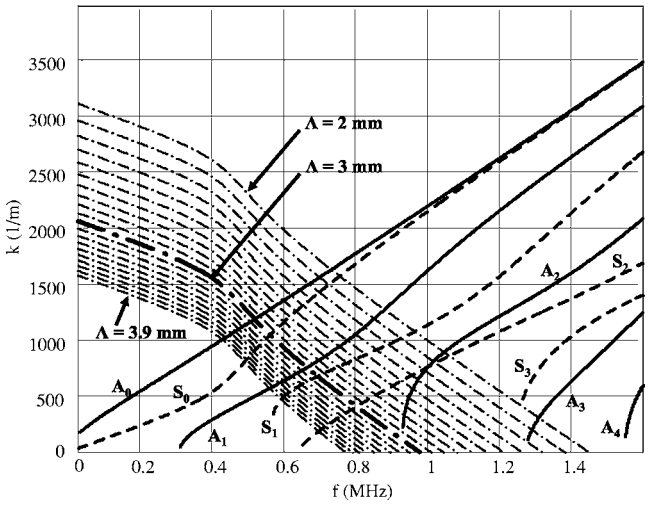

FIG. 4. Theoretical dispersion curves for the studied aluminium plates: solid lines for antisymmetric modes and dotted lines for symmetric modes. For each studied spatial periodicity, curves resulting from the phonon relation [Eq. (2)] are plotted in dashed-dotted lines.

A grating with ten grooves and a spatial periodicity of 3.7 mm is studied with depths varying from $p=50$ to 400 μm. Whatever the value of p, the wave number related to the converted mode always corresponds to the S_2 reflected mode (Fig. 5), where level one corresponds to the amplitude of the incident mode. We note that the amplitude of the S_2 mode increases with the value of p. If the depth is low compared to the Lamb wave wavelength and the plate thickness ($p<200$ μm), the amplitude of the S_2 mode is proportional to the depth of the grooves. The evolution for $p>200$ μm could be interpreted by a different distribution of the energy of the incident wave among more reflected waves (an S_0 converted-reflected mode is observed). In this case, the phonon relation involving only the S_2 reflected mode is not sufficient to describe the interaction of the Lamb waves with the periodical grating.

For a given depth, the amplitude of the reflected mode increases with the number of grooves.

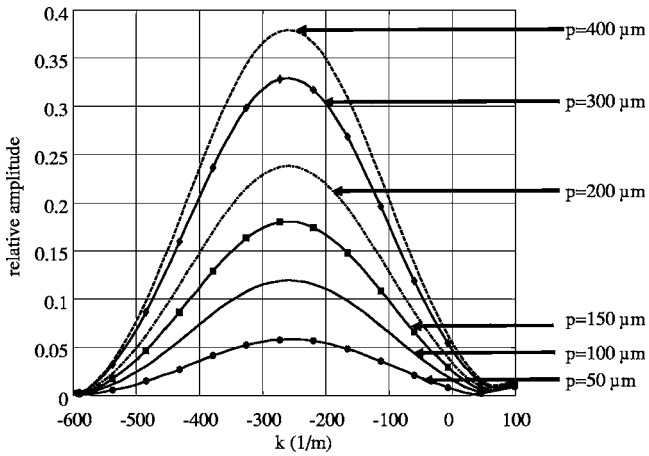

FIG. 5. Representation of the wave number related to the S_2 converted mode for various depths in dual space (k,f). The grating contains ten grooves. The spatial periodicity is equal to $\Lambda=3.7$ mm.

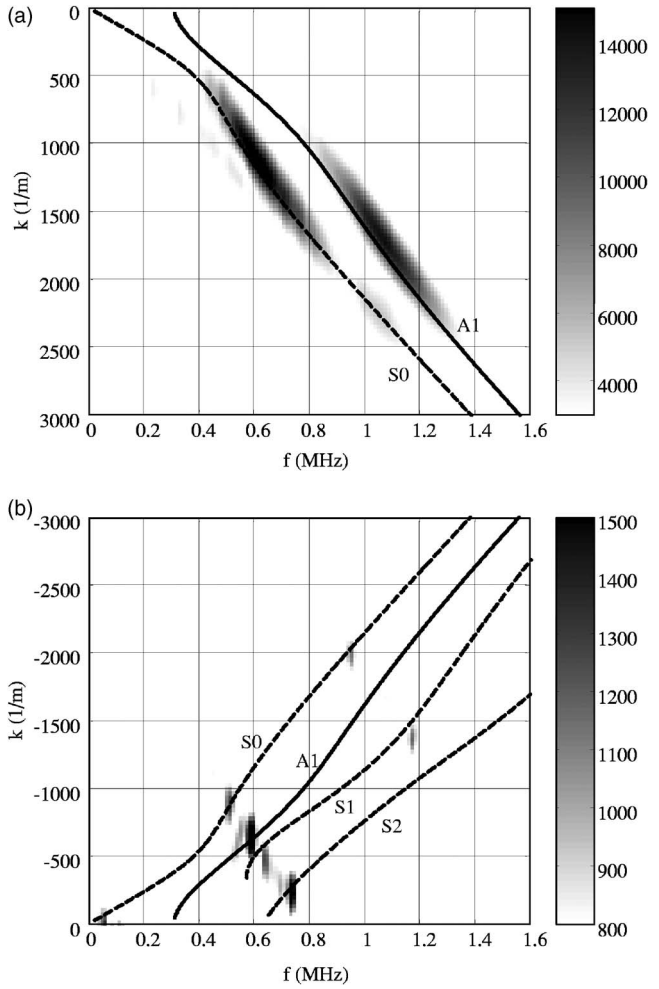

FIG. 6. (a) Representation of the experimental incident signal in dual space (k,f). (b) Representation of the experimental reflected signal in dual space (k,f).

IV. EXPERIMENTAL RESULTS

The experimental setup is the following. A pulse generator delivers a very short pulse voltage (about 300 V during a period of 300 ns) to a piezo-composite transducer. The central frequency of this emitting transducer is 1 MHz. Lamb waves are then generated by the wedge method with a wedge angle of 49° to excite the S_0 mode around a frequency equal to 800 kHz. The characteristics of the experimental grating are groove depth p equal to 100 μm and spatial periodicity of the grooves Λ equal to 3.7 mm. An optical profilometer is used to characterize the surface of the sample. The root mean square value (rms) $R_q=29.2$ μm is obtained.

The S_0 wave is generated on a flat area. Then the wave is propagated over 18 mm before reaching the grating. A noncontact detection is done using a laser vibrometer: it measures the normal surface displacement of the plate along the principal direction of propagation by 0.1 mm steps. For each spatial position, the amplitude is recorded and allows us to obtain an (x,t) image similar to Fig. 2 obtained in the FEM study. The evolution of the amplitude in the different modes is plotted as a function of the distance.

The S_0 wave is generated on the [430–850 kHz] frequency range [Fig. 6(a)]. Four reflected converted modes are obtained at different frequencies [Fig. 6(b)]: three reflected converted modes (A_1,S_1,S_2) and one nonconverted reflected mode (S_0). The corresponding wave-number values are reported in Table II. The phonon relation is verified with a maximum error of 2.5%. The S_2 converted mode is experimentally found at $f=730$ kHz. It was numerically found at $f=710$ kHz, using the FEM analysis (Table I). The small discrepancy is due to the acoustical parameters, which are slightly different in the experimental part and in the numerical study. For each conversion, the phonon relation is well verified.

TABLE II. Comparison between the sum of the incident (k_{S0}) and reflected-converted wave numbers (k_{A1},k_{S1},k_{S2}) and reflected (k_{S0}) and the phonon wave number related to the grating ($2\pi/\Lambda$). The column "frequency" corresponds to the frequency of the conversion.

	Incident	Reflected mode						
Frequency (kHz)	k_{S0} (1/m)	k_{S2} (1/m)	k_{S1} (1/m)	k_{A1} (1/m)	k_{S0} (1/m)	Σk (1/m)	$2\pi/\Lambda$ (1/m)	Relative error
730	1455	230				1685	1698	0.8%
635	1180		475			1655	1698	2.5%
585	1040			650		1690	1698	0.5%
515	815				875	1690	1698	0.5%

V. CONCLUSIONS

Incident Lamb waves propagating in a plate with a periodic grating are converted into reflected modes. A phonon relation is written between the incident signal, the converted mode and the phonon related to the grating.

The spatial periodicity of the grating determines the frequency of the converted modes, whereas the depth of the grooves only modifies the amplitude of the converted modes. Therefore, for the cases presented in this paper, the effects of the spatial periodicity of the grating and the groove depth are independent. Experiment and numerical results are in good agreement.

Future works will consist in studying surface profile with several spatial periodicities in order to have a more accurate representation of a rough surface.

ACKNOWLEDGMENTS

This work is supported by the research group on ultrasonics (GDR CNRS No. 2501, France). The authors would like to thank Philippe Saint-Martin (IUT, Le Havre, France) for machining experimental samples and Dawn Hallidy for proofreading the manuscript.

[1] J. A. Ogilvy, "Wave scattering from rough surfaces," Rep. Prog. Phys. **50**, 1553–1608 (1987).
[2] M. De Billy and G. Quentin, "Backscattering of acoustic waves by randomly rough surfaces of elastic solids immersed in water," J. Acoust. Soc. Am. **72**, 591–601 (1982).
[3] O. I. Lobkis and D. E. Chimenti, "Elastic guided waves in plates with surface roughness. I. Model calculation," J. Acoust. Soc. Am. **102**, 143–149 (1997).
[4] O. I. Lobkis and D. E. Chimenti, "Elastic guided waves in plates with surface roughness. II. Experiments," J. Acoust. Soc. Am. **102**, 150–159 (1997).
[5] D. Leduc, B. Morvan, P. Pareige, and J.-L. Izbicki, "Measurement of the

effects of rough surfaces on Lamb wave propagation," NDT & E Int. **37**, 207–211 (2004).
[6]C. Potel, D. Leduc, B. Morvan, P. Pareige, J. L. Izbicki, and C. Depollier, "Lamb wave propagation in isotropic media with rough interface: comparison between theoretical and experimental results," in *Proceedings of the World Congress on Ultrasonics* (ISBN 2-9515619-9-7, CD-ROM ISBN 2-9521105-0-6), Paris, France (2003), Vol. 2, pp. 609–612.
[7]C. Potel, D. Leduc, B. Morvan, P. Pareige, C. Depollier, and J.-L. Izbicki, "Propagation of Lamb waves in anisotropic rough plates: a perturbation method," in *Proceedings of the French Congress on Acoustic* (CFA/DAGA'04—ISBN 2-9521105-1-4, CD-ROM ISBN 2-9521105-3-0), Strasbourg, France (2004), Vol. 1, pp. 147–148.
[8]J. M. Clayes, O. Leroy, A. Jungman, and L. Adler, "Diffraction of ultrasonic waves from periodically rough liquid-solid surfaces," J. Appl. Phys. **54**(10), 5657–5662 (1983).
[9]K. Mampaert and O. Leroy, "Reflection and transmission of normally incident ultrasonic waves on periodic solid-liquid interfaces," J. Acoust. Soc. Am. **83**, 1390–1398 (1988).
[10]W. Lauriks, L. Kelders, and J. F. Allard, "Surface waves above gratings having a triangular profile," Ultrasonics **36**, 865–871 (1998).
[11]A. Jungman, L. Adler, J. D. Achenbach, and R. Roberts, "Reflection from a boundary with periodic roughness: theory and experiment," J. Acoust. Soc. Am. **74**, 1025–1032 (1983).
[12]J. R. Chamuel, "Transient Scholte wave transmission along rough liquid/solid interfaces," J. Acoust. Soc. Am. **83**, 1336–1344 (1988).
[13]H. Duflo, A. Tinel, and J. Duclos, "Scholte wave propagation and diffraction on a fluid/solid periodic rough surface," in *Proceedings of the I.E.E.E. International Ultrasonics Symposium* (ISBN 0-7803-2012-3), Cannes, France (1994), pp. 719–722.
[14]ATILA® Finite Element Code for Piezoelectric and Magnetostrictive Transducer Modeling, Version 5.2.1, User's Manual, ISEN, Acoustics Laboratory, Lille, France (2002).